

## Particle injections with auroral expansions

K. Liou, C.-I. Meng, P. T. Newell, and A. T. Y. Lui

Applied Physics Laboratory, Johns Hopkins University, Laurel, Maryland

G. D. Reeves and R. D. Belian

Los Alamos National Laboratory, Los Alamos, New Mexico

**Abstract.** We compare the onset of dispersionless energetic particle injections, observed as a sudden increase of energetic (tens to hundreds of keV) electron and ion fluxes on a timescale of  $\sim 1$  min, with the start of auroral breakups. A total of 34 dispersionless injections observed by Los Alamos National Laboratory (LANL) satellites are analyzed, and their corresponding auroral breakups are determined with global auroral images acquired from the Polar ultraviolet imager. An important finding is that dispersionless injections can actually be associated with substorm intensification. The injection time at LANL relative to the start of auroral breakups varies from -2 to 8 min and can sometimes be more than 10 min. The average lag time for the injections compared to the auroral breakups is 1.8 min with a standard deviation of 2.5 min. It is suggested that particle energization must take place in the magnetotail  $\sim 1$  min earlier than the start of the explosive auroral substorm onset, while the delay of the injections at LANL is due to a propagation effect. An implied average earthward injection boundary is estimated to be  $\sim 6.9 - 9.2 R_E$ . Further analysis of the delay time indicates that the transport of substorm injections is associated with the enhancement of convection electric field by a factor of  $\sim 5$ , corresponding to an earthward convection flow speed of  $5 - 120 \text{ km s}^{-1}$ . Dispersionless injections can take place in a fairly wide magnetic local time (MLT) region from 2000 to 0100 MLT with a peak at 2200 MLT, where auroral breakups occur most frequently. More importantly, dispersionless injections have ionospheric footprints clustered around the location of auroral breakup within  $\pm 1$  hour of MLT, further supporting the concept of the close relationship between the substorm injections and the auroral breakups.

### 1. Introduction

The injection of plasma and energetic particles near the inner edge of the plasma sheet, also known as a substorm injection, is one of the fundamental signatures of magnetospheric substorm [Arnoldy and Chan, 1969; McIlwain, 1974]. The characteristic feature of the substorm injection is a sharp increase in electron and proton fluxes of a wide range of energies, usually from

tens to hundreds of keV, over their presubstorm levels. When the enhancement of particle fluxes occurs at different energies simultaneously, the injection is called a "dispersionless injection."

The injection region is located at a distance ranging from  $4.3$  to  $15 R_E$  tailward of the Earth [Friedel *et al.*, 1996]. This region is significant in magnetospheric substorm physics because substorm onset arcs map along the Earth's magnetic field lines to this re-

gion [Murphree *et al.*, 1993] and the initiation of substorm current wedge occurs in the near-Earth region from  $\sim 6$  to  $10 R_E$  [Lui, 1991; Kennel, 1992]. Dispersionless substorm injections are frequently observed in the premidnight sector [Lopez *et al.*, 1990], where auroral breakups most frequently occur [Craven and Frank, 1991; Liou *et al.*, 2000b], and are associated with the formation of substorm current wedge, which also frequently takes place in the premidnight sector [Lopez *et al.*, 1990]. This close association of the substorm injections with many substorm onset signatures has made the injections one of the most reliable substorm onset indicators. Kamide and McIlwain [1974] examined five large noticeable substorm events and reported that particle injections were observed at synchronous orbit in association with every substorm they surveyed. However, there was a considerably large difference of 8 min, on average, between the two onset signatures. While this discrepancy may be due primarily to the large uncertainty in determining the substorm onset time from the ground magnetograms, dispersionless particle injections may sometimes show a delay relative to auroral breakups [Liou *et al.*, 1999].

There are various substorm signatures frequently used to time the onset of magnetospheric substorm. These signatures include high-latitude, negative magnetic bays; low-latitude Pi2 pulsations [Rostoker, 1968; Saito *et al.*, 1976]; dispersionless, energetic particle injections at geosynchronous orbit [Saito *et al.*, 1976; Belian *et al.*, 1981; Reeves *et al.*, 1997]; intensification of auroral kilometric radiation (AKR) [Slavin *et al.*, 1993; Murata *et al.*, 1995]; and the auroral breakups [Akasofu, 1964]. Recently, Liou *et al.* [1998a, 1999] reported that these popular onset indicators do not always occur at the same time, and, in general, most of the substorm onset indicators were found to lag behind the auroral breakup as determined with global auroral images. Although based on a few events, these studies have called attention to the issue of substorm onset timing. More recently, Liou *et al.* [2000a] studied 119 low-latitude Pi2 pulsations and showed a typical  $\sim 1 - 3$  min delay of the Pi2 onsets relative to the auroral breakups, supporting their previous case study results.

Earlier, Liou *et al.* [1999] reported a 1 - 3 min delay of the dispersionless energetic electron and proton injections with respect to the auroral breakups. One should not be surprised by the small delay of the injections relative to the auroral breakups, since the injection source is not always local to the observers. However, we would like to stress that this kind of delay has not been recognized by the community, and it can be evident from the

common use of geosynchronous injections for substorm onsets in numerous reported papers. For this reason, we have conducted a statistical study to compare the relative timing of the dispersionless substorm injections at geostationary orbit and the auroral breakups to show the typical time difference between the two onsets. We will provide a possible mechanism that controls the time difference between the two substorm onset signatures. The longitudinal distribution of the dispersionless injection will also be examined.

## 2. Observations

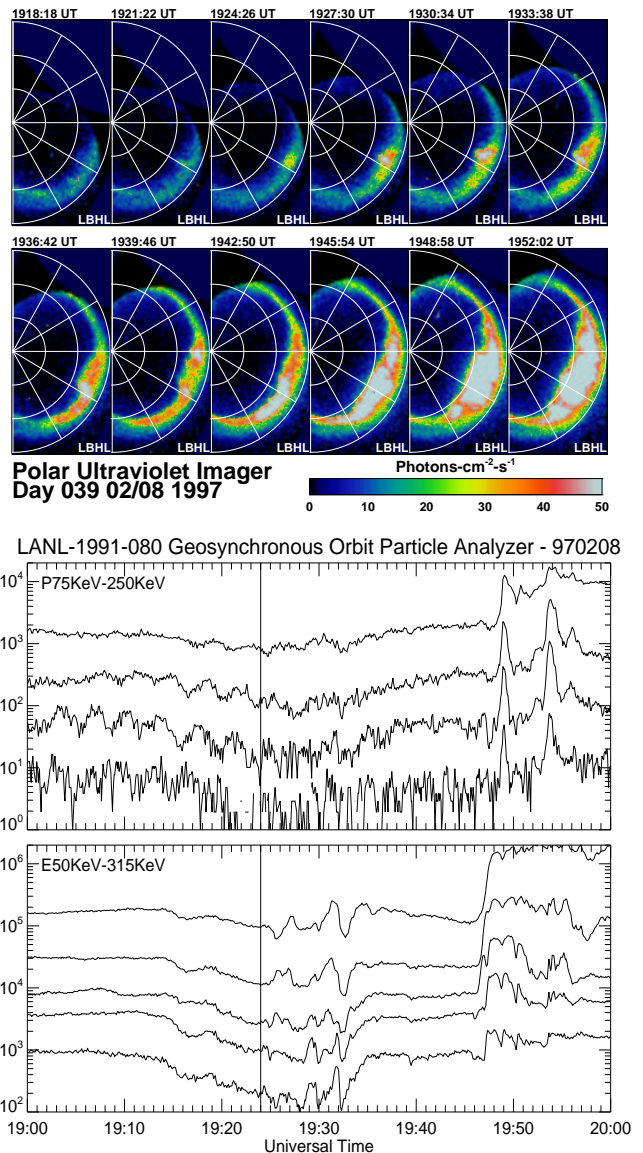
For the purpose of this study a reliable substorm onset time is required. To achieve this goal, we will use global auroral images acquired from the Polar ultraviolet imager (UVI) [Torr *et al.*, 1995] instead of the narrow field-of-view all-sky imager to identify auroral breakups. One of the apparent advantages of using a global auroral imager, such as UVI, to identify substorm onsets is its capability of resolving the space-time aliasing problem inherent in single point measurements. UVI is capable of providing continuous coverage of most of the northern auroral oval at a temporal resolution of  $\sim 37$  s. Energetic electron and proton data from synchronous orbit particle analyzer (SOPA) on board the Los Alamos National Laboratory (LANL) 1994-084 and the LANL 1991-080 spacecraft [see, e.g., Belian *et al.*, 1992] will be used to determine injection events. The temporal resolution for SOPA is 10 s, and thus it can time the injection reliably within  $\pm 10$  s.

We have searched the SOPA database from April 1996 to May 1997 and from December 1997 to April 1998 for injection events for the time periods when the UVI images are available. The selection criterion is that either electron (50-315 keV) or proton (75 - 400 keV) injections must be seen as dispersionless on a timescale of  $\sim 1$  min. Very often the observed injections display dispersive signatures since particles may undergo energy-dependent gradient-curvature drifts after injections. Although it is still possible to trace injection particles back to their source and get a good timing of the injection [Belian *et al.*, 1978; Reeves *et al.*, 1991], a dispersive type of injection is avoided in the present study to simplify the timing procedure for injection. In addition, selections of dispersionless injection automatically establish the location of the injection region as being local or early to the observer. On the basis of this criterion, we have identified 34 dispersionless injection events with simultaneous UVI auroral observations. The injection time for these events is determined either by electron

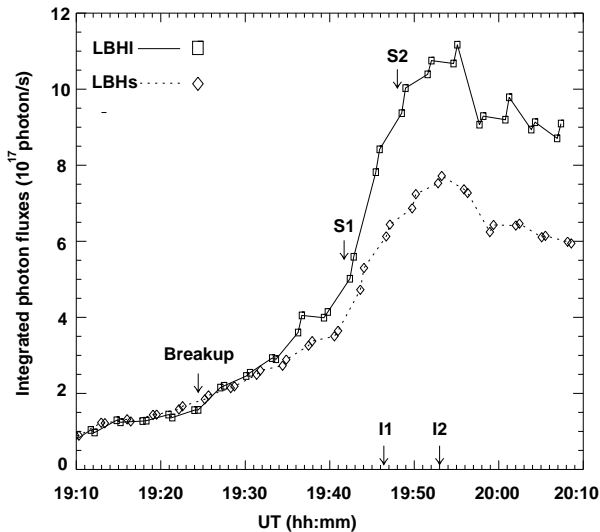
or by proton injections, whichever occur first, and the injection time is compared to the auroral breakup determined from the UVI images. Actually, most of the selected events have both electron and ion injections simultaneously. One of the events will be discussed below in detail.

Plate 1 (top) shows a sequence of false color Polar UVI auroral images accumulated over 36 s in the long Lyman-Birge-Hopfield bands (160 – 180 nm) for a large substorm event on February 8, 1997. The planetary  $K_p$  index increased from 2- to 6- after the substorm onset, indicating a very large substorm event. The time tag indicates the center of the integration interval. Auroral images are mapped to the usual magnetic local time-latitude format, based on the Altitude Adjusted Corrected Geomagnetic Coordinates (AACGM) coordinates [Baker and Wing, 1989]. A sudden brightening of auroras with intensity of  $\sim 30$  photon  $\text{cm}^{-2} \text{s}^{-1}$ , corresponding to a precipitating electron energy flux of  $\sim 8$  ergs  $\text{cm}^{-2} \text{s}^{-1}$ , can be identified at  $\sim 2220$  magnetic local time (MLT) and  $62.5^\circ$  magnetic latitude (Mlat) at 1924:26 UT. By examining images of the highest time resolution (not shown), we confirm that the auroral breakup occurred between 1923:58 and 1924:26 UT. An enhancement of plasma waves in the AKR band was also observed at  $\sim 1924$  UT by the Polar plasma wave observations. There were a couple of intensifications of aurora at  $\sim 1942$  and  $\sim 1948$  UT. The first intensification was associated with a new onset surge centered at  $\sim 2130$  MLT, and the second but less pronounced intensification was associated with a surge centered at  $\sim 2300$  MLT that expanded eastward and poleward. The integrated photon flux over the auroral bulge is shown in Figure 1 in which the auroral breakup and the two intensifications (S1 and S2) can be identified.

The energetic proton and electron data observed by the LANL 1991-080 satellite for the substorm interval is plotted in Plate 1 (bottom). The LANL 1991-080 satellite, which had an ionospheric footprint of 2345 MLT and  $62.9^\circ$  Mlat at the onset time ( $\sim 1$  hour east of the breakup arcs), did not observe any injection until 1946:24 UT for electrons and 1948:12 UT for protons, more than a 20 min delay from the auroral breakup. From the sequence of auroral images (Plate 1, top) one can see that the eastward edge of the substorm auroral bulge did not reach the MLT of the LANL 1991-080 footprint until  $\sim 12$  min later at  $\sim 1936:42$  UT. Large variations in electron channels were seen during this time but not at injection level. After  $\sim 1942$  UT (first intensification) the poleward edge of the auroral bulge reached the LANL footprint and beyond, and a few min-



**Plate 1.** (top) A sequence of nightside LBHL auroral images from Polar ultraviolet imager showing auroral breakups at 1924:26 UT on February 8, 1997. The time tag indicates the center time of each snapshot accumulated in 36 s. The latitude ( $10^\circ$  increments) and magnetic local time (2-hour increments; dusk at the bottom of each frame, and midnight to the right of each frame) are in Altitude Adjusted Corrected Geomagnetic Coordinates (AACGM) coordinates. (bottom) Energetic proton and electron data observed by LANL 1991-080 for the 1900 - 2000 UT period on February 8, 1997.



**Figure 1.** Integrated photon fluxes over an area defined by  $60^\circ - 75^\circ$  magnetic latitude (Mlat) and 2000 - 0200 magnetic local time (MLT) for a portion of substorm period between 1910 and 2010 UT on February 8, 1997, from Polar ultraviolet imager (UVI) observations. The down-arrow indicates the time when the first auroral brightening in association with the breakup was identified. Two auroral intensifications (S1 and S2) and two geosynchronous particle injections (I1 and I2) are also marked at appropriate times

utes later the injections from both electrons and protons occurred. Therefore these electron and ion injections are likely to be associated with the first intensification of the substorm auroral bulge at  $\sim 1942$  UT. The slightly leading electron injection indicates that the center of the injection is to the west of the LANL 1991-080 and is consistent with the center location of the new auroral surge observed by UVI. A second dispersionless injection (ion only) was seen at  $\sim 1953$  UT. It cannot be associated with proton drift echoes [cf. *Belian et al.*, 1978], because the protons of the second from the top curve, for example (110-170 keV), will have a drift period of roughly 40 min and would appear at  $\sim 2025$  UT (off Plate 1). Therefore this second injection is likely to be associated with another auroral intensification at 1948:58 UT. Assuming the two injections initiated from a similar distance from the Earth, the  $\sim 6$  min separation of the two injections is consistent with the time separation of the two auroral intensifications.

How often does this kind of delay occur at geosynchronous orbit? This question is answered by Figure 2 in which the occurrences of the dispersionless injections are organized with respect to the time difference between the injections and the auroral breakups (i.e., the

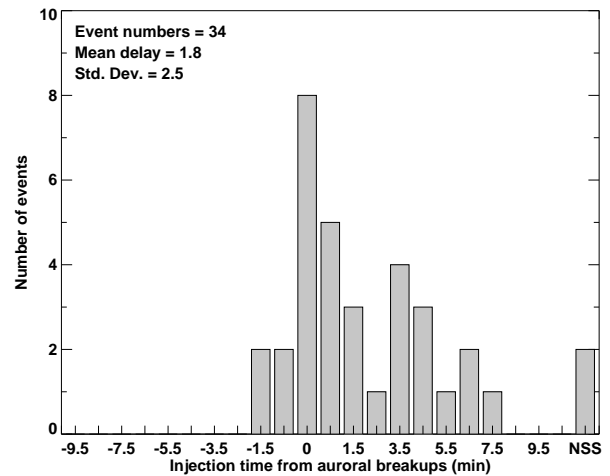


**Figure 2.** Occurrence rates of the dispersionless substorm injections as a function of the time difference between the injections and the auroral breakups.

injection time is subtracted from the start of the auroral breakup). The time difference between the two types of onset are widely scattered from -2 to 8 min. There are much more delay (positive bins) events than lead (negative bins) injection events. The average delay time is 1.8 min with a large standard deviation of 2.5 min. The 95% confidence interval from a simple statistic  $t$ -test on the distribution mean is (0.9, 2.7) min. It should be noted that we found two injection events with a delay time greater than 10 min. These events are indicated by “NSS” in Figure 2.

### 3. Discussion

Dispersionless energetic particle injections have been considered as one of the most reliable substorm indicators and are often used to precisely time the onset of substorms. However, less attention has been given to the fact that as long as observations are not made locally to the injection source, there will always be a delay. The question is how much delay is typical at geosynchronous orbit. On the basis of 34 events, it is found that the dispersionless injections seen at geosynchronous orbit tend to lag behind the auroral breakups by an average of  $1.8 \pm 2.5$  min. For some events the delay is greater than 5 min. The particular event shown in Plate 1 clearly indicates that dispersionless injections can be associated with substorm intensification. This particular event and many others also indicate that substorm injections were seen when the substorm auroral bulge expands over the ionospheric footprint of the LANL satellite. Therefore substorm surges may actually be the ionospheric signature of magnetospheric

substorm injections, and the equatorward edge of the substorm surge may correspond to the injection front. A detailed analysis of this possible relationship is undertaken to understand the ionospheric signature of the substorm injections.

An interesting finding is that dispersionless injections can sometimes be seen at geosynchronous orbit  $\sim 1$  min earlier than the start of corresponding auroral breakups. This suggests that at the beginning of a substorm energy dissipation process, particle energization, probably associated with a current disruption [e.g., *Fairfield and Ness, 1970*], takes place in the magnetotail first. The cross-tail current is diverted as a field-aligned current into and out of the auroral ionosphere with the speed of Alfvén waves. This 1 - 2 min time is consistent with a round trip of Alfvén transit time. The delay of dispersionless substorm injections seen by LANL relative to the start of the corresponding auroral breakup simply reflects the finite time propagation of the substorm-energized plasma flow which is nonlocal to the LANL orbit.

Although there are many proposed models aiming to explain the acceleration mechanism, the basic discrepancy among them is whether the acceleration is local or nonlocal. The dispersionless feature of energetic particle flux increases seems to provide evidence for their local acceleration. However, a local acceleration cannot explain the highly scattered delay time. Therefore it is likely that the acceleration takes place at a remote site and propagates toward the Earth. Indeed, radially inward propagation of dispersionless injections has been observed by two radially separated satellites [*Moore et al., 1981*]. The varying delay time indicates a varying acceleration location. In order to preserve the dispersionless feature of injection down to the geostationary orbit, a dawn-to-dusk electric field is needed. Indeed, electric fields between  $L = 2.5$  and  $L = 8.5$  in the local time sector between 1200 and 0400 MLT are nearly always duskward [*Rowland and Wygant, 1998*]. A primarily duskward tail electric field, associated with a fast flow that jets earthward, has been demonstrated by MHD simulations by *Birn et al. [1998]*. Their simulation results suggest a large inductive electric field at the leading edge of the fast flow. More recently, *Fok et al. [1999]* calculated test particle trajectories in an induced electric field, associated with substorm magnetic variations (i.e., field line stretching and dipolarization), superposed upon a background global convection electric field; *Fok et al.* showed that substorm injection seen at the nightside geosynchronous orbit is associated with an earthward motion of a heated plasma region with

a sharp earthward boundary similar to those reported by *McIlwain [1974]* and *Mauk and Meng [1983]*. On the other hand, it is also possible that the background magnetic configuration is altered by a compressed magnetic field structure propagating earthward [*Russell and McPherron, 1973*] in a sense to reduce the curvature and gradient of the local magnetic field. This possibility is confirmed by *Li et al. [1998]*, whose test particle simulation results are able to reproduce the observations.

On the basis of the above discussion, it is reasonable to conclude that the delay time of the dispersionless injection seen at geosynchronous orbit relative to the auroral breakup is associated with the transport of the plasma from the energization regions, and this delay time can be used to infer the earthward injection boundary. A schematic representation of the injection and auroral breakup is given in Figure 3. If we take the typical bursty plasma transport velocity to be  $\sim 100 \text{ km s}^{-1}$  [*Baumjohann et al., 1988, 1989; Moore et al., 1981*] and the Alfvén transit time to be 30 s, an average dispersionless injection delay time of  $\sim 1.8 \pm 2.5$  min suggests an average earthward injection boundary of  $\sim 9.2 \pm 3.3 R_E$ . This boundary can be just outside of the geosynchronous orbit at  $\sim 6.9 \pm 0.3 R_E$  if we take the lower end of the plasma convection speed reported by *Moore et al. [1981]* into consideration. Interestingly, in situ particle observations have also indicated that the injection regions are located at distances ranging from  $x = -4.3$  to  $x = -15 R_E$  [*Friedel et al., 1996*]. This region is where magnetic field lines on which auroral breakups typically map (average  $x = -7.8 R_E$ ) [*Murphree et al., 1993*] and tail current disruptions frequently occur ( $8.8 - 12 R_E$ ) [*Ohtani et al., 1992; Ohtani, 1998*]. It is important to note that if the injection is produced at substorm onset, our result favors substorm models suggesting a near-Earth initiation of substorm. There are a few instances indicating that dispersionless substorm injections occur at or even earlier than auroral breakups. This indicates that substorm onsets must take place right at the LANL satellite locations. It also suggests that particle energization actually precedes auroral breakup, but that time delays to propagate to geosynchronous cause the latter to lag.

Since substorm injections often take place tailward of the geosynchronous orbit and take a finite time to transport earthward, the varying delay time should be determined not only by the radial distance of the injection source but also by the plasma flow speed. To validate this argument, we use the  $y$  component of the solar wind electric field as a proxy of the duskward electric field in the tail region [*Lei et al., 1981*]. The (hourly)

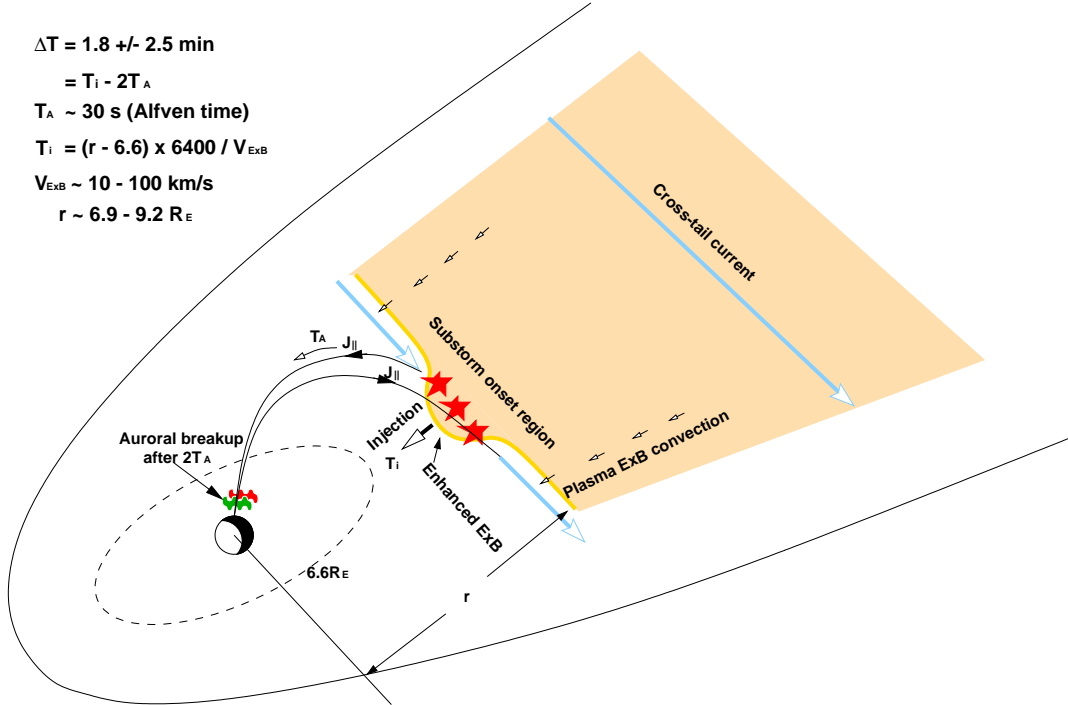


**Figure 3.** Schematic representation of the relationship between injections and auroral breakups.

solar wind electric field is obtained from the product of the  $x$  component of the solar wind and the  $z$  component of the Interplanetary Magnetic Field (IMF) from the Wind observations that are averaged over a 1-hour period prior to the substorm onsets. A proper time delay is estimated by taking the observed solar wind velocity and the IMF into account [Liou *et al.*, 1998b]. We divide the 32 events into two groups according to the relative radial locations of the LANL satellite and the auroral breakup. The auroral breakup locations for the 32 events are first mapped to the magnetospheric equatorial plane by using the empirical model of *Tsyganenko* [1989, hereinafter referred to as T89].

For auroral breakups earthward of LANL (Figure 4a), a small correlation coefficient (C.C.) of -0.03 is obtained, indicating that the delay time is not likely controlled by the convection velocity. This is not surprising because injections taking place at or earthward of the LANL orbit will move away from the LANL. Indeed, the delay is small, close to 0, for most of the events. For this kind of event the delay time of the substorm injection is probably determined by the tailward expansion of the injection source. On the other hand, when the auroral breakups are tailward of the LANL (Figure 4b), the correlation coefficient is considerably much higher

(C.C. = -0.75). This suggests that a smaller time delay (including negative delay) is associated with a stronger convection flow.

It has been shown that the duskward electric field in the magnetotail is positively correlated with the  $y$  component of the solar wind electric field [Lei *et al.*, 1981]. Therefore a sudden increase in electron and ion fluxes at substorm onset is likely to be local, and their presence at geosynchronous orbit is due to an enhanced earthward convection of the plasma in the near-Earth magnetotail [Birn *et al.*, 1997; Fok *et al.*, 1999]. A high correlation coefficient seems to imply that all the surveyed injections originated from a rather limited near-Earth region. In addition, a larger cross-tail electric field will move the magnetotail and injection boundary closer to the Earth and hence reduce the delay time as well. To counter this problem, we use the plasma sheet footprint of the auroral breakup as the injection source to calculate the distance from the LANL. The plasma convection associated dawn-to-dusk electric is estimated by using an empirical formula,  $E_M$  ( $\text{mV m}^{-1}$ ) =  $0.09 + 0.13 E_y$  ( $\text{mV m}^{-1}$ ), derived by Lei *et al.* [1981], and the magnetic field was two-point averaged on the basis of the T89 model magnetic field at the injection region and the LANL location. Then we can derive the

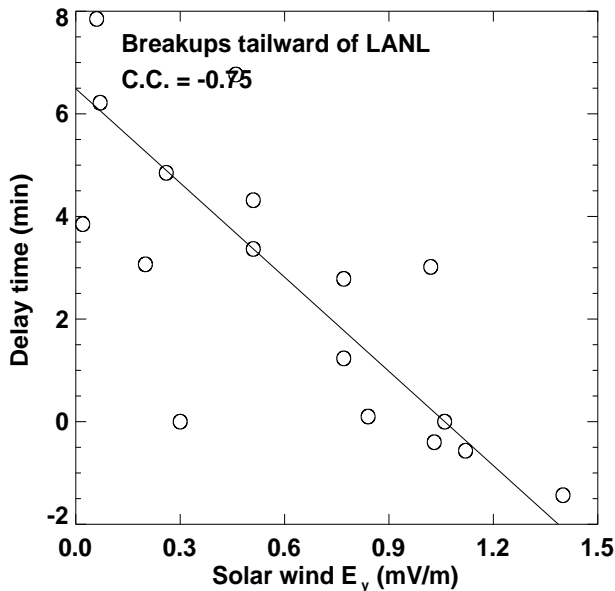
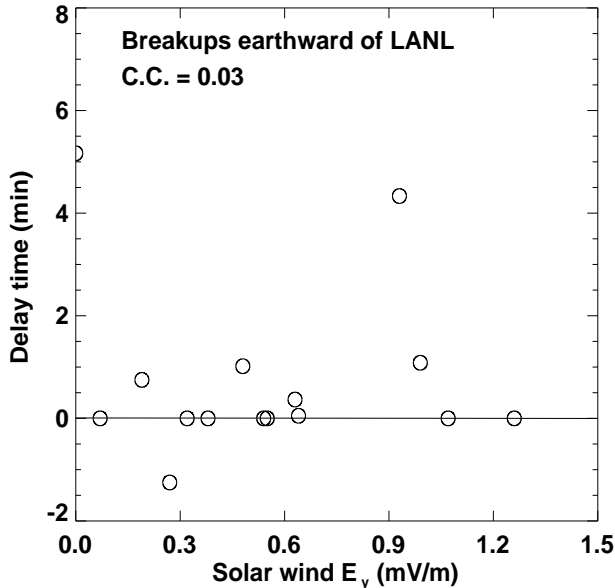


**Figure 4.** Delay time of the dispersionless substorm injections relative to the auroral breakups as a function of the solar wind electric field ( $E_y = B_z \times V_x$ ) for breakups occurring (a) earthward of the LANL and (b) tailward of the LANL.

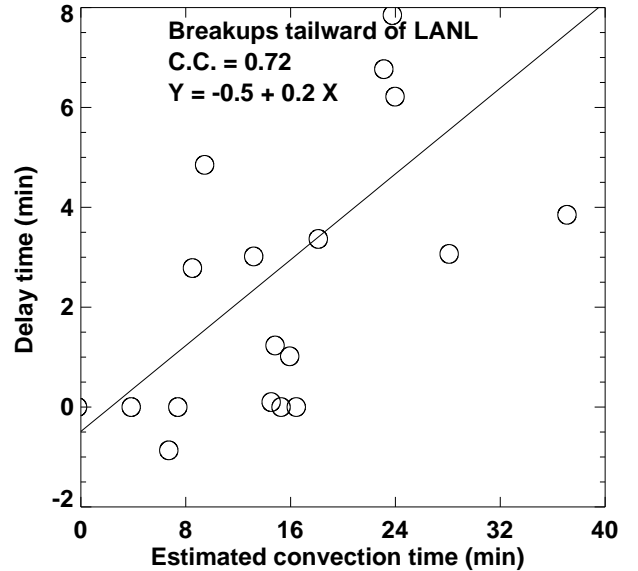


**Figure 5.** Dispersionless substorm injection delay time versus the estimated delay time inferred from an empirical formula,  $E_M$  ( $\text{mV m}^{-1}$ ) =  $0.09 + E_y$  [Lei et al., 1981], where  $E_y$  is the solar wind electric field.

plasma  $E \times B$  drift speed and estimate the propagation time by dividing the relative distance between the injection and LANL by the convection speed. The result is shown in Figure 5 with a good correlation (C.C. = 0.72). The estimated delay time, defined by the estimated convection time minus 1 min, is found to be  $\sim 5$  times larger than the observed delay time. In order to match the propagation time with the delay time, the electric field must be increased by a factor of  $\sim 5$ , corresponding to an earthward flow of propagation speed of  $\sim 5 - 120 \text{ km s}^{-1}$ . The earthward expansion velocity of the injection boundary has been measured previously by utilizing two radially separated satellites by Russell and McPherron [1973] ( $150 \text{ km s}^{-1}$ ), Moore et al. [1981] ( $10 - 100 \text{ km s}^{-1}$ ), and Ohtani [1998] (one event at  $180 \text{ km s}^{-1}$  and one at  $30 \text{ km s}^{-1}$ ), though in situ measurements can sometimes overestimate the expansion speed when the two satellites are not aligned along the expansion direction. Note that the correlation coefficient is not improved from the one with an assumed fixed injection location. This is probably because there are large uncertainties in the field line mapping, because T89 is a 3-hour-averaged magnetic field model that cannot represent the highly changing magnetic field configuration during substorm periods.

The longitudinal distribution of dispersionless par-

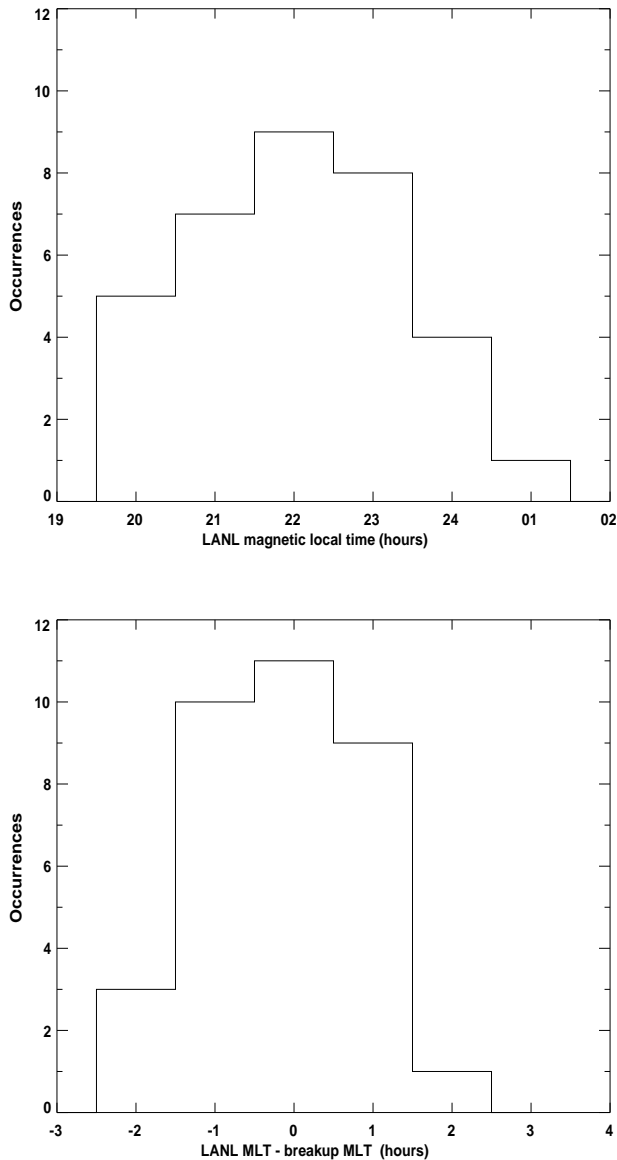


**Figure 6.** Occurrence rates of surveyed substorm events ordered by the (a) MLT of the LANL satellite and the (b) relative MLT locations of the LANL to the auroral breakups.

ticle injection has been studied by *Lopez et al.* [1990], who analyzed 167 substorm-associated, dispersionless (on a timescale of 1.5 min) ion injections and found that ion injections occurred preferentially in the pre-midnight region but peak at midnight. They attributed this local time asymmetry to the westerly drift of energetic ions injected near the midnight sector. We argue that this local time asymmetry is most likely due to the fact that substorms occur most frequently in the pre-midnight sector [e.g., *Craven and Frank, 1991; Liou et al., 2000b*] because their injection events were dispersionless. To show this possibility, we have plotted the longitudinal distribution of the 34 substorm injection events in Figure 6a. From Figure 6a, dispersionless injections can be observed from 2000 to 0100 MLT with a peak at 2200 MLT. If the distribution is plotted in terms of the relative MLT location of the injections to the auroral breakups (see Figure 6b), the injections are found to cluster around the local time of the auroral breakups. The average longitudinal width of the dispersionless substorm injections is  $\sim 2$  hours in MLT and is consistent with the previous findings of 1 hour from *Reeves et al.* [1992] and 3 hours from *Arnoldy and Moore* [1983]. This result suggests that the center of dispersionless injection coincides with the center of auroral breakup.

#### 4. Conclusions

We have compared the relative timing of the two most important substorm onset signatures, dispersionless energetic particle injections at geosynchronous orbit and auroral breakups. It is shown that the time difference between the two onsets is highly scattered. The onset of a dispersionless injection lags behind the corresponding auroral breakup by  $1.8 \pm 2.5$  min, on average, although the delay can be more than 5 min. This implies an average earthward injection boundary of  $\sim 9.2 \pm 3.3 R_E$  for a maximum propagation speed of  $100 \text{ km s}^{-1}$  for the injection plasma. Although the radial distance of the injection location from the observational site should determine the delay time, results surprisingly indicate that larger earthward convection velocity, inferred from the  $y$  component of the solar wind magnetic field, leads to a smaller delay. An enhanced earthward flow speed of  $5 - 120 \text{ km s}^{-1}$  during the injection process is needed to account for the observed delay time. The surveyed dispersionless injection events were observed in a wide range of magnetic local time from 2000 to 0100 MLT with a peak at 2200 MLT, coinciding with the general distribution of the auroral breakup occurrences. Importantly, the dispersionless injections

were found to cluster within  $\pm 1$  hour from the MLT location of the auroral breakups.

**Acknowledgments.** R. D. Belian is the principal investigator for the SOPA on board the LANL 1994-084 satellite, and G. Parks is the principal investigator for the ultraviolet imager on board the Polar satellite. This work was supported by NASA grants NAG 5-7724 and NAG 5-9078 and NSF grant ATM 9819805 to the Johns Hopkins University Applied Physics Laboratory.

Janet G. Luhmann thanks Alfred Vampola and another referee for their assistance in evaluating this paper.

## References

- Akasofu, S.-I., The development of the auroral substorm, *Planet. Space Sci.*, *12*, 273, 1964.
- Arnoldy, R. L., and T. E. Moore, The longitudinal structure of substorm injections at synchronous orbit, *J. Geophys. Res.*, *88*, 6213, 1983.
- Arnoldy, R. R., and K. W. Chan, Particle substorms observed at the geostationary orbit, *J. Geophys. Res.*, *74*, 5019, 1969.
- Baker, K. B., and S. Wing, A new coordinate system for conjugate studies at high latitudes, *J. Geophys. Res.*, *94*, 9139, 1989.
- Baumjohann, W., G. Paschmann, N. Sckopke, C. A. Cattell, and C. W. Carlson, Average ion moments in the plasma sheet boundary layer, *J. Geophys. Res.*, *93*, 11,507, 1988.
- Baumjohann, W., G. Paschmann, and C. A. Cattell, Average plasma properties in the central plasma sheet, *J. Geophys. Res.*, *94*, 6597, 1989.
- Belian, R. D., D. N. Baker, P. R. Higbie, and E. W. J. Hones, High resolution energetic particle measurements at  $6.6 R_E$ , *J. Geophys. Res.*, *83*, 4857, 1978.
- Belian, R. D., D. N. Baker, E. W. J. Hones, P. R. Higbie, S. J. Bame, and J. R. Asbridge, Timing of energetic proton enhancements relative to magnetospheric substorm activity and its implication for substorm theories, *J. Geophys. Res.*, *86*, 1415, 1981.
- Belian, R. D., G. R. Gisler, T. E. Cayton, and R. A. Christensen, High-Z energetic particles at geosynchronous orbits during the great solar proton event series of October, 1989, *J. Geophys. Res.*, *97*, 16,897, 1992.
- Birn, J., M. F. Thompson, J. E. Borovsky, G. D. Reeves, D. J. McComas, and R. D. Belian, Characteristic plasma properties during dispersionless substorm injection at geosynchronous orbit, *J. Geophys. Res.*, *102*, 2309, 1997.
- Birn, J., M. F. Thomsen, J. E. Borovsky, G. D. Reeves, D. J. McComas, R. D. Belian, and M. Hesse, Substorm electron injections: Geosynchronous observations and test particle simulations, *J. Geophys. Res.*, *103*, 9235, 1998.
- Craven, J. D., and L. A. Frank, Diagnosis of auroral dynamics using global auroral imaging with emphasis on large-scale evolution, in *Auroral Physics*, edited by C.-I. Meng, M. J. Rycroft, and L. A. Frank, p 273, Cambridge Univ. Press, New York, 1991.
- Fairfield, D. H., and N. F. Ness, Configuration of the geomagnetic tail during substorms, *J. Geophys. Res.*, *75*, 7032, 1970.
- Fok, M.-C., T. E. Moore, and D. C. Delcourt, Modeling of inner plasma sheet and ring current during substorms, *J. Geophys. Res.*, *104*, 14,557, 1999.
- Friedel, R. H. W., A. Korth, and G. Kremser, Substorm onset observed by CRESS: Determination of energetic particle source region, *J. Geophys. Res.*, *101*, 13,137, 1996.
- Kamide, Y., and C. E. McIlwain, The onset time of magnetosphere substorms determined from ground and synchronous satellite records, *J. Geophys. Res.*, *79*, 4787, 1974.
- Kennel, C., The kiruna conjecture: The strong version, in *Proceedings of the International Conference on Substorms (ICS-1)*, Eur. Space Agency Spec. Publ., ESA SP-335, 599, 1992.
- Lei, W., R. Gendrin, B. Higel, and J. Berchem, Relationships between the solar wind electric field and the magnetospheric convection electric field, *Geophys. Res. Lett.*, *8*, 1099, 1981.
- Li, X., D. N. Baker, M. Temerin, G. D. Reeves, and R. D. Belian, Simulation of dispersionless injections and drift echoes of energetic electrons associated with substorms, *Geophys. Res. Lett.*, *25*, 3759, 1998.
- Liou, K., C.-I. Meng, A. T. Y. Lui, P. T. Newell, M. Brittnacher, G. Parks, and M. Nosé, A fresh look at substorm onset identifiers, in *Substorms-4*, edited by S. Kokubun and Y. Kamide, p. 249, Kluwer Acad., Norwell, Mass., 1998a.
- Liou, K., P. T. Newell, C.-I. Meng, A. T. Y. Lui, M. Brittnacher, and G. Parks, Characteristics of the solar wind controlled auroral emissions, *J. Geophys. Res.*, *103*, 17,543, 1998b.
- Liou, K., C.-I. Meng, A. T. Y. Lui, P. T. Newell, M. Brittnacher, G. Parks, G. D. Reeves, R. R. Anderson, and K. Yumoto, On relative timing in substorm onset signatures, *J. Geophys. Res.*, *104*, 22,807, 1999.
- Liou, K., C.-I. Meng, P. T. Newell, K. Takahashi, S.-I. Ohtani, A. T. Y. Lui, M. Brittnacher, and G. Parks, Evaluation of low-latitude  $\Pi_2$  pulsations as indicators of substorm onset using Polar ultraviolet imagery, *J. Geophys. Res.*, *105*, 2495, 2000a.
- Liou, K., P. T. Newell, D. G. Sibeck, C.-I. Meng, M. Brittnacher, and G. Parks, Observation of IMF and seasonal effects in the location of auroral substorm onset, *J. Geophys. Res.*, *in press*, 2000b.
- Lopez, R. E., D. G. Sibeck, R. W. McEntire, and S. M. Krimigis, The energetic ion substorm injection boundary, *J. Geophys. Res.*, *95*, 109, 1990.
- Lui, A. T. Y., A synthesis of magnetospheric substorm models, *J. Geophys. Res.*, *96*, 1849, 1991.
- Mauk, B. H., and C.-I. Meng, Characterization of geostationary particle signatures based on the "injection boundary" model, *J. Geophys. Res.*, *88*, 3055, 1983.
- McIlwain, C. E., Substorm injection boundaries, in *Magnetospheric Physics*, edited by B. M. McCormac, p. 143, D. Reidel, Norwell, Mass., 1974.

- Moore, T. E., R. L. Arnoldy, J. Feynman, and D. A. Hardy, Propagating substorm injection fronts, *J. Geophys. Res.*, *86*, 6713, 1981.
- Murata, T., H. Matsumoto, H. Kojima, A. Fujita, T. Nagai, T. Yamamoto, and R. R. Anderson, Estimation of tail reconnection lines by AKR onsets and plasmoid entries observed with Geotail spacecraft, *Geophys. Res. Lett.*, *22*, 1849, 1995.
- Murphree, J. S., R. D. Elphinstone, M. G. Henderson, L. L. Cogger, and D. J. Hearn, Interpretation of optical substorm onset observations, *J. Atmos. Terr. Phys.*, *55*, 1159, 1993.
- Ohtani, S., Earthward expansion of tail current disruption: Dual-satellite study, *J. Geophys. Res.*, *103*, 6815, 1998.
- Ohtani, S., S. Kokubun, and C. T. Russell, Radial expansion of the tail current disruption during substorms: A new approach to the substorm onset region, *J. Geophys. Res.*, *97*, 3129, 1992.
- Reeves, G. D., R. D. Belian, and T. A. Fritz, Numerical tracing of energetic particle drifts in a model magnetosphere, *J. Geophys. Res.*, *96*, 13,997, 1991.
- Reeves, G. D., G. Kettmann, T. A. Fritz, and R. D. Belian, Further investigation of the CDW 7 substorm using geosynchronous particle data: Multiple injections and their implications, *J. Geophys. Res.*, *97*, 6417, 1992.
- Reeves, G. D., R. D. Belian, T. C. Cayton, M. G. Henderson, R. A. Christensen, P. S. McLachlan, and J. C. Ingraham, Using Los Alamos geosynchronous energetic particle data in support of other missions, in *Satellite-Ground Based Coordinate Source Book*, edited by M. Lockwood et al., *Eur. Space Agency Spec. Publ.*, *SP-1198*, 263, 1997.
- Rostoker, G. A., Macrostructure of geomagnetic bays, *J. Geophys. Res.*, *73*, 4217, 1968.
- Rowland, D. E., and J. R. Wygant, Dependence of the large-scale, inner magnetospheric electric field on geomagnetic activity, *J. Geophys. Res.*, *103*, 14,959, 1998.
- Russell, C. T., and R. L. McPherron, Semiannual variation of geomagnetic activity, *J. Geophys. Res.*, *78*, 92, 1973.
- Saito, T., K. Yumoto, and Y. Koyama, Magnetic pulsation Pi2 as a sensitive indicator of magnetospheric substorm, *Planet. Space Sci.*, *24*, 1025, 1976.
- Slavin, J. A., M. F. Smith, E. L. Mazur, D. N. Baker, J. E. W. Hones, T. Iyemori, and E. W. Greenstadt, ISEE 3 observations of traveling compression regions in the Earth's magnetotail, *J. Geophys. Res.*, *98*, 15,425, 1993.
- Torr, M. R., et al., A far ultraviolet imager for the international solar-terrestrial physics mission, *Space Sci. Rev.*, *71*, 329, 1995.
- Tsyganenko, N. A., A solution of the Chapman-Ferraro problem for an ellipsoidal magnetopause, *Space Sci. Rev.*, *71*, 329, 1989.
- R. D. Belian and G. D. Reeves, Los Alamos National Laboratory, Los Alamos, NM 87545. (rdbelian@lanl.gov; reeves@lanl.gov)
- K. Liou, A. T. Y. Lui, C.-I. Meng, and P. T. Newell, The Johns Hopkins University Applied Physics Laboratory, Laurel, MD 20723. (kan.liou@jhuapl.edu; anthony.lui@jhuapl.edu; ching.meng@jhuapl.edu; patrick.newell@jhuapl.edu)

Received March 7, 2000; revised May 8, 2000; accepted May 9, 2000.

---

This preprint was prepared with AGU's L<sup>A</sup>T<sub>E</sub>X macros v5.01, with the extension package 'AGU++' by P. W. Daly, version 1.6b from 1999/08/19.